A Complexity-Reduced 2D Behavioral Modeling Configuration for the Linearization of Concurrent Dual-Band Transmitters

Manel Chouchane[1], Marouan Othmani[1], and Noureddine Boulejfen[2]
[1]Faculty of Sciences of Tunis, University of Tunis El Manar, Tunis, Tunisia
[2]Military Research Center, Tunis, Tunisia

Abstract
This paper proposes a complexity-reduced 2D memory polynomial model (MPM) for the linearization of concurrent dual-band radio transmitters. The proposed model presents a new configuration of a 2D MPM to be used for the modeling and digital predistortion (DPD) of power amplifiers (PAs). The presented technique alleviates the oversizing issue faced in the conventional 2D model by separating the highly nonlinear memoryless and mildly nonlinear dynamic behaviors, which results in a smaller number of coefficients, and therefore, reduced computational complexity is achieved. With the measurement setup, the proposed model achieved relatively the same performance as the conventional formulation while significantly reducing the model dimension by about 50%. The experiments were carried out using two 5G new radio (NR) signals with a bandwidth of 20 MHz and a PAPR of 8 dB each.
Keywords: *Behavioral modeling, digital predistortion, dual-band, memory polynomial model, power amplifier*

1. Introduction

Radio frequency (RF) transmitters' front-ends play a critical role in the operation of the telecommunication link. More specifically, the RF power amplifier (PA) has the most significant impact on the performance of the overall transmitter system. Recent wireless telecommunication technologies are more and more employing higher data rates to fulfill the requirements of speed, resolution, etc. This is achieved by employing high-order constellations and more advanced access techniques. As a result, the generated signals vary rapidly and have a high peak-to-average power ratio (PAPR) [1], [2]. Therefore, the PA should be backed off from the saturation region, which results in low-efficiency operation. To improve the efficiency without compromising the linearity performance, adopting a linearization technique becomes a necessity.

The main linearization techniques are feedback, feedforward, and digital predistortion (DPD) [1]-[3]. There has been a great deal of research recently on the use of the DPD linearization technique. DPD consists of including the inverse behavioral model of the PA in the transmitter before the actual nonlinear component. As a result, the cascade of the inverse behavioral model and the PA would be a linearized system [2]-[13]. However, when dealing with dual-band transmitters, single-band DPDs are not practical in this regard due to the neglected cross-modulation effects that appear between the two modulated signals, or due to that appear between the two modulated signals, or due to the important sampling rate requirements for the employed digital-to-analog converters (DACs) and analog-to-digital converters (ADCs).

A solution has been introduced in [14] to design a 2D DPD for the linearization of concurrent dual-band transmitters. This technique consists of designing a 2D memory polynomial model (MPM) that enables dealing with each band separately [14], [15]. Moreover, the 2D MPM enables considering the cross-modulation effects between the two signals. In the developed model in [14], both modulated signals contribute to predicting the PA's behavior for each band. However, due to the nested summations in the mathematical expression of the 2D MPM, the number of coefficients increases significantly with the increase of the nonlinearity order and/or the memory depth of the model.

In this paper, we propose a new complexity-reduced 2D MPM for the linearization of concurrent dual-band transmitters. The proposed model consists of a new configuration of the 2D MPM that enables to significantly reduce the number of coefficients, and therefore, reduced complexity and better matrix conditioning are achieved. In fact, the proposed model mitigates the oversizing issue of the conventional model by dealing with the nonlinearity order and memory branches more efficiently, which enables achieving the same performance with less complexity.

This paper is organized as follows. In section II, we present an overview of the conventional memory polynomial modeling techniques for the single- and dual-band cases. Section III introduces the proposed complexity-reduced 2D MPM. In section IV, the measurement setup used in this work is described. Section V presents and analyses the obtained measurement results. Finally, the conclusion is given in section VI.

2. Principle of the Memory Polynomial Model

2.1 Single-Band Memory Polynomial Model

The nonlinearity of the PA can be theoretically modeled using the well-known memory polynomial model, which is formulated as follows

Manuscript received March 5, 2022
Manuscript revised March 20, 2022
https://doi.org/10.22937/IJCSNS.2022.22.3.61

$$y(n) = \sum_{m=0}^{M} \sum_{k=1}^{K} a_{m,k} x(n-m)|x(n-m)|^{k-1} \quad (1)$$

where $x(n)$ and $y(n)$ are the complex input and output baseband waveforms, respectively; K is the nonlinearity order; M is the memory depth; $a_{m,k}$ are the complex memory polynomial coefficients. The block diagram of the MPM is illustrated in Fig. 1.

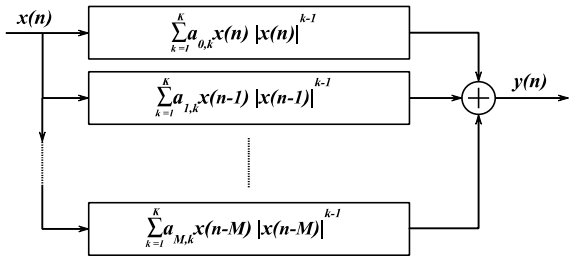

Fig. 1. Block diagram of the memory polynomial model.

The nonlinear behavior of the PA generates distortions that cause spectral regrowth at the transmitter's output, and linearization techniques, such as DPD, are therefore needed. The inverse model can be determined based on expression (1) in order to compensate for the nonidealities of the nonlinear device.

The nonlinear behavior of the PA is more noticeable when dealing with two signals, in which the carrier frequencies are separated by $\Delta\omega$ and transmitted simultaneously. In this case, using a single DPD system requires processing the whole bandwidth of the signal captured at the output of the PA. The main limitation of this approach is the sampling rate requirements of the ADCs. In addition, using two independent DPDs with the conventional MPM for compensation of distortions in each frequency band is not appropriate since the cross-modulation effect is not considered in this approach.

.

2.2 Dual-Band Memory Polynomial Model

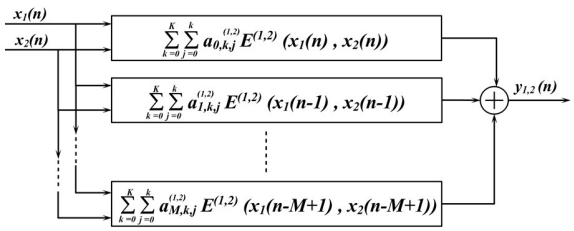

Fig. 2. Block diagram of the 2D MPM.

A two-input model has been introduced in [14] to deal with concurrent dual-band transmitters. In this model, the PA is modeled using two input signals, which are captured and digitized separately. This technique takes into consideration the effect of the cross-modulation between the two signals and enables processing each band independently, which improves the accuracy and reduces the sampling rate requirement. The 2D MPM reads as follows

$$y_1(n) = \sum_{m=0}^{M-1} \sum_{k=0}^{K} \sum_{j=0}^{k} a_{m,k,j}^{(1)} x_1(n-m) \times |x_1(n-m)|^{k-j} |x_2(n-m)|^{j} \quad (2)$$

$$y_2(n) = \sum_{m=0}^{M-1} \sum_{k=0}^{K} \sum_{j=0}^{k} a_{m,k,j}^{(2)} x_2(n-m) \times |x_2(n-m)|^{k-j} |x_1(n-m)|^{j} \quad (3)$$

where $x_1(n)$ and $x_2(n)$ are the complex baseband envelopes of the RF input signals at the upper and lower signal bands, respectively; $y_1(n)$ and $y_2(n)$ are the captured complex baseband envelopes at the same bands; $a_{m,k,j}^{(1)}$, and $a_{m,k,j}^{(2)}$ are the model coefficients; K and M are the nonlinearity order and the memory depth, respectively.

Expressions (2) and (3) can be represented in a more general form as follows

$$y_{1,2}(n) = \sum_{m=0}^{M-1} \sum_{k=0}^{K} \sum_{j=0}^{k} a_{m,k,j}^{(1,2)} E^{(1,2)}\big(x_1(n-m), x_2(n-m)\big) \quad (4)$$

The block diagram of the conventional 2D MPM is shown in Fig. 2 using expression (4).

2.3 Limitations of the conventional 2D model

As it can be noticed by observing the expressions (2) and (3), the number of coefficients increases rapidly with the increase of the order and/or the memory branches due to the existence of the nested summations in the model, leading to a higher computational complexity for the digital processing. Furthermore, the conventional model assumes that the nonlinearity order of the static part is equal to the nonlinearity order of the dynamic part. This leads to an over-dimensioned model as the number of coefficients would be more than needed, which causes numerical stability issues due to the ill-conditioning of the observation matrix.

3. Proposed Complexity-Reduced 2D Model

The proposed configuration is based on decoupling the contribution of the static and dynamic behaviors of the PA. This configuration consists of identifying the highly nonlinear static and mildly nonlinear dynamic behaviors of the PA separately. Then, the outputs are added to build the

estimated signal. The parallel 2D model is expressed as follows

$$y_1(n) = \sum_{p=0}^{K_s}\sum_{h=0}^{p} a_{p,h}^{(1)} x_1(n)|x_1(n)|^{p-h}|x_2(n)|^h + \sum_{m=0}^{M-1}\sum_{l=0}^{K_d}\sum_{r=0}^{l} b_{m,l,r}^{(1)} x_1(n-m)|x_1(n-m)|^{l-r}|x_2(n-m)|^r \quad (5)$$

$$y_2(n) = \sum_{p=0}^{K_s}\sum_{h=0}^{p} a_{p,h}^{(2)} x_2(n)|x_2(n)|^{p-h}|x_1(n)|^h + \sum_{m=0}^{M-1}\sum_{l=0}^{K_d}\sum_{r=0}^{l} b_{m,l,r}^{(2)} x_2(n-m)\ |x_2(n-m)|^{l-r}|x_1(n-m)|^r \quad (6)$$

where K_s and K_d are the model nonlinearity orders for the highly nonlinear static and mildly nonlinear dynamic parts, respectively; $a_{p,h}^{(1,2)}$ and $b_{m,l,r}^{(1,2)}$ are the corresponding complex coefficients.

Expressions (6) and (7) can be reformulated as

$$y_1(n) = \sum_{p=0}^{K_s}\sum_{h=0}^{p} a_{p,h}^{(1,2)} E^{(1,2)}\big(x_1(n), x_2(n)\big) + \sum_{m=0}^{M-1}\sum_{l=0}^{K_d}\sum_{r=0}^{l} b_{m,l,r}^{(1,2)} F^{(1,2)}\big(x_1(n-m), x_2(n-m)\big) \quad (7)$$

Therefore, the corresponding block diagram of the proposed model would be as represented in Fig. 3.

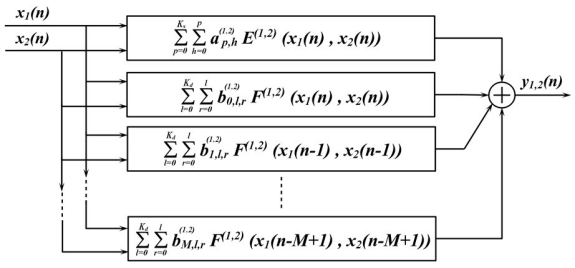

Fig. 3. Block diagram of the proposed model.

The separation between the highly nonlinear static behavior and mildly nonlinear dynamic behavior solves the complexity issues related to the conventional 2D model and gives better modeling distribution. Therefore, the high nonlinearity order K_s is applied only once, whereas K_d will be the one applied equally for all the memory branches. The new configuration reduces significantly the number of coefficients, and therefore, reduced complexity and improved observation matrix properties are achieved.

4. Measurement Setup

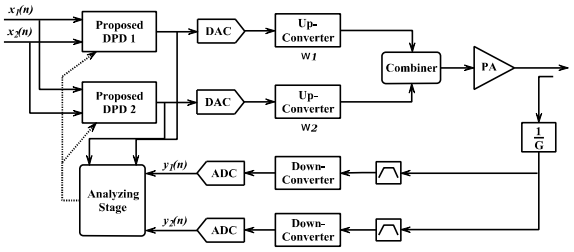

Fig. 4. Principle of the DPD linearization technique used in this work.

Fig. 4 shows the DPD linearization principle used in this work. The system uses two transmission channels for the lower and upper frequency bands, respectively. Each channel has its own predistorter, which is based on the proposed model. After being pre-distorted, the digital signal of each channel passes through a digital-to-analog converter (DAC) and then up-converted to a specific carrier frequency. After that, the resulted RF signals are combined to be boosted by the PA. To estimate the DPD coefficients, a portion of the amplified signal is attenuated and fed back to the digital processor after being separated, down-converted, and then digitized. The digital processor unit calculates the DPD parameters and updates the main predistorter.

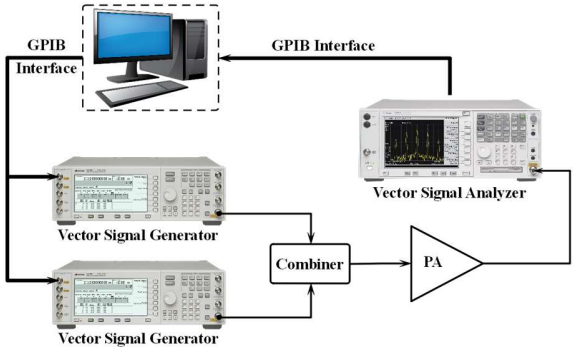

Fig. 5. Measurement setup used in this work.

The measurement setup used for the evaluation of the proposed modeling technique is described in Fig. 5. First, a computer running MATLAB generates two 5G NR signals with a bandwidth of 20 MHz and a PAPR of 8 dB each. The generated complex waveforms are then sent to two vector signal generators (VSGs), where the signals are modulated and up-converted. The resulted RF signals are combined by an RF combiner and then fed to the power amplification unit. For forward and inverse modeling, the amplified RF signals are captured separately using two band-pass filters centered at ω_1 and ω_2. These signals are then down-converted and

digitized by a vector signal analyzer (VSA), to be sent to the computer to perform gain normalization and time alignment between the received and input data. In the case of DPD, the normalized output signal is used as model input, and the input signal is used as output to achieve the inverse modeling. Finally, the estimated coefficients of each module are copied to the predistorter. The DACs and ADCs were designed in MATLAB using delta-sigma modulators (DSMs).

5. Measurement Results

The performance assessments were done to evaluate the proposed technique from modeling and linearization points of view.

For the forward modeling performance, we used the number of coefficients to determine the complexity of the model and the normalized mean square error (NMSE) to measure the accuracy of modeling. The NMSE is commonly used for the evaluation of PAs' behavioral models. This metric can be calculated using the following expression

$$\mathrm{NMSE} = 10\log_{10}\left(\frac{\sum_{l=1}^{L}|y_{measured}(l) - y_{estimated}(l)|^2}{\sum_{l=1}^{L}|y_{measured}(l)|^2}\right) \quad (8)$$

where $y_{measured}(l)$ is the measured output of the PA; $y_{estimated}(l)$ is the estimated output of the model; L is the length of the time domain waveforms.

First, Fig. 6 shows how the number of coefficients significantly increases with the increase of the nonlinearity order, which can cause stability issues, especially for PAs with high nonlinearity orders or memory depth.

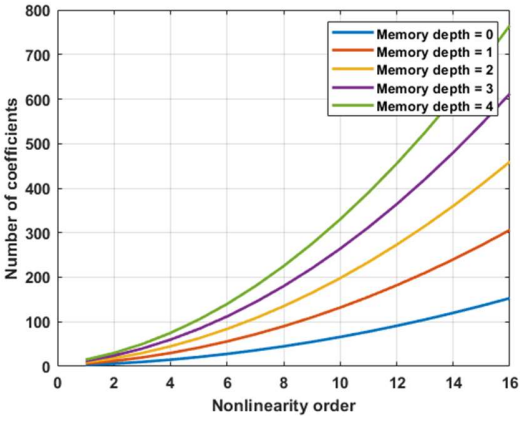

Fig. 6. Number of coefficients in function of the nonlinearity order for different memory depth values.

In order to measure the forward modeling performance, Table 1 summarizes the NMSE and the number of coefficients of the introduced model compared to the conventional 2D MPM. The proposed model was able to achieve an NMSE close to the one of the conventional 2D MPM with a reduced number of coefficients to about 50%. These results prove that the proposed configuration significantly reduces the complexity of the system while maintaining the accuracy of modeling.

Table 1. Forward modeling results of the conventional and proposed 2D models

Model	NMSE	Number of coefficients
Conventional 2D MPM	-43.14	273
Proposed 2D MPM	-43.02	136

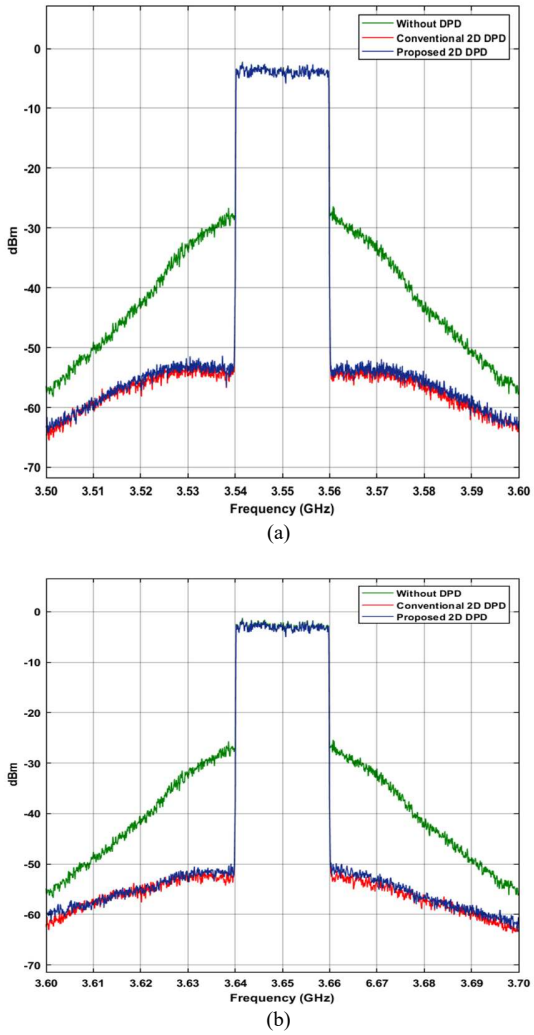

Fig. 7. Output spectra of the conventional and proposed DPDs. (a) Lower band. (b) Upper band.

Table 2. Summary of the ACPR and AltCPR of the conventional and proposed 2D DPDs for the lower frequency band

DPD	ACPR (dBc)		AltCPR (dBc)	
	Lower band	Upper band	Lower band	Upper band
Without DPD	-28.86/-29.15	-28.91/-29.12	-45.20/-45.45	-44.86/-45.04
Conventional 2D DPD	-50.91/-51.35	-50.47/-51.49	-55.59/-56.26	-54.94/-57.07
Proposed 2D DPD	-50.01/-50.45	-49.78/-50.38	-55.23/-55.43	-54.67/-56.42

Regarding the linearization performance, we used the adjacent channel power ratio (ACPR) and alternate channel power ratio (AltCPR) metrics to measure the spectral regrowth of the designed DPDs. The ACPR and AltCPR are the comparisons between the average powers of the adjacent and alternate channels, and the average power of the amplified channel. These metrics are defined as

$$\text{ACPR(dBc)} = 10\log_{10}\left(\frac{P_{adj}}{P_{chann}}\right) \quad (9)$$

and

$$\text{AltCPR(dBc)} = 10\log_{10}\left(\frac{P_{alt}}{P_{chann}}\right) \quad (10)$$

where P_{adj} and P_{alt} are the powers of the adjacent and alternate channels, respectively, and P_{channe} is the power of the main channel.

The obtained spectra for the lower and upper frequency bands are reported in Fig. 7. It can be observed that the proposed and conventional systems were able to enormously reduce the spectral regrowth caused by the PA nonlinearity. Furthermore, both DPD systems have provided close performances. This is confirmed in Table 2 which summarizes the ACPRs and AltCPRs of the evaluated DPDs. These results prove that the proposed configuration outperforms the conventional 2D DPD technique while significantly reducing the complexity of the system.

6. Conclusion

This paper proposes a new configuration of a 2D MPM that reduces the complexity of modeling while achieving the same performance. In fact, the proposed model solves the oversizing issue of the conventional 2D MPM. The introduced configuration significantly reduces the number of coefficients, and therefore, reduced hardware complexity and enhanced stability are achieved. The technique consists of separating the highly nonlinear static behavior from the mildly nonlinear behavior, which leads to a better coefficients distribution without oversizing problems. The presented model was evaluated and compared to the conventional 2D MPM using a commercial PA. The obtained results have shown reduced complexity of the proposed technique with close modeling and linearization performances.

References

[1] S. Cripps, *RF Power Amplifiers for Wireless Communications, Second Edition*, 2006.

[2] B. Lathi and Z. Ding, *Modern Digital and Analog Communication Systems*, ser. Oxford Series in Electrical an. Oxford University Press, 2009.

[3] A. Katz, J. Wood, and D. Chokola, "The evolution of pa linearization: From classic feedforward and feedback through analog and digital predistortion," *IEEE Microwave Magazine*, vol. 17, no. 2, pp. 32 –40, 2016.

[4] S. A. Bassam, M. Helaoui, and F. M. Ghannouchi, "2-d digital predistortion (2-d-dpd) architecture for concurrent dual-band transmitters," *IEEE Transactions on Microwave Theory and Techniques*, vol. 59, no. 10, pp. 2547–2553, 2011.

[5] S. A. Bassam, W. Chen, M. Helaoui, F. M. Ghannouchi, and Z. Feng, "Linearization of concurrent dual-band power amplifier based on 2 d-dpd technique," *IEEE Microwave and Wireless Components Letters*, vol. 21 , no. 12, pp. 685–687, 2011.

[6] K. Muhonen, M. Kavehrad, and R. Krishnamoorthy, "Look-up table techniques for adaptive digital predistortion: a development and comparison," *IEEE Transactions on Vehicular Technology*, vol. 49, no. 5 , pp. 1995–2002, 2000.

[7] W. Cao, S. Wang, P. N. Landin, C. Fager, and T. Eriksson, "Complexity optimized digital predistortion model of rf power amplifiers," *IEEE Transactions on Microwave Theory and Techniques*, pp. 1–1, 2021.

[8] C. Yu, L. Guan, E. Zhu, and A. Zhu, "Band-limited volterra seriesbased digital predistortion for wideband rf power amplifiers," *IEEE Transactions on Microwave Theory and Techniques*, vol. 60, no. 12 , pp. 4198–4208, 2012.

[9] P. Song, Z. Mokhti, and Q. Mu, "Investigation on a desirable dpd architecture and trapping characteristics for gan power amplifier linearization," in *2021 IEEE MTT-S International Microwave Symposium (IMS)*, 2021, pp. 531–533.

[10] X. Xia, Y. Liu, C. Li, W. Guo, C. Shi, S. Shao, L. Lei, and Y. Tang, "A high-accuracy digital predistorter constructed by reproducing iterations of ilc with cascade architecture," in *2021 IEEE MTT-S International Microwave Symposium (IMS)*, 2021, pp. 446–449.

[11] ——, "A high-accuracy digital predistorter constructed by reproducing iterations of ilc with cascade architecture," in *2021 IEEE MTT-S International Microwave Symposium (IMS)*, 2021, pp. 446–449.

[12] W. Chen, S. Zhang, Y.-J. Liu, F. M. Ghannouchi, Z. Feng, and Y. Liu, "Efficient pruning technique of memory polynomial models suitable for pa behavioral modeling and digital predistortion," *IEEE Transactions on Microwave Theory and Techniques*, vol. 62, no. 10, pp. 2290–2299 , 2014.

[13] Z. Liu, X. Hu, L. Xu, W. Wang, and F. M. Ghannouchi, "Low computational complexity digital predistortion based on convolutional neural network for wideband power amplifiers," *IEEE Transactions on Circuits and Systems II: Express Briefs*, pp. 1–1, 2021.

[14] Z. Xu, Q. Zhang, L. Zhang, Z. Yu, C. Yu, and J. Zhai, "Iterative learning control for digital predistortion with undersampled feedback signal," *in 2021 IEEE MTT-S International Wireless Symposium (IWS)*, 2021, pp. 1 – 3.

[15] A. Zhu, "Decomposed vector rotation-based behavioral modeling for digital predistortion of RF power amplifiers," *IEEE Transactions on Microwave Theory and Techniques*, vol. 63, no. 2, pp. 737–744 , 2015.